Multi-site phosphorylation of the TOPBP1 ATR Activation Domain propels ATR signaling during the response to DNA breaks

Holly Senebandith[1], Kenna Ruis[1], Katrina Montales[1], Oanh Huynh[1], Yasaman Jami-Alahmadi[2], James A. Wohlschlegel[2], and W. Matthew Michael[1,3]

[1]Molecular and Computational Biology Section
Department of Biological Sciences
University of Southern California
Los Angeles, CA 90089

[2]Department of Biological Chemistry
Geffen School of Medicine at UCLA
Los Angeles, CA 90095

[3]Author for correspondence at: mattm@usc.edu

Abstract

TOPBP1 is a BRCT domain-containing scaffold protein that plays important roles in a diverse array of cellular processes, including DNA damage signaling, DNA repair, DNA replication, and mRNA transcription. For DNA damage signaling, TOPBP1 activates the crucial damage response kinase ATR and this occurs during replication stress as well as during a DNA double-strand break response. ATR signaling allows cells to survive genotoxic issues and represents a formidable barrier to transformation to a tumorigenic state. Despite its importance to genome stability, the biochemical mechanism for how TOPBP1 activates ATR is not fully understood. TOPBP1 uses a discrete domain, termed the ATR activation domain, to stimulate ATR kinase. Recent work has shown that the AAD must be in a multimeric state to activate ATR. Other work has shown that phosphorylation of the AAD on serine 1131 (in Xenopus) is important for its function, and some have suggested that this is linked to the formation of TOPBP1 condensates during a DNA damage response. In this study we examine AAD phosphorylation in detail and we report three important new findings. One, S1131 phosphorylation promotes ATR activation in a manner independent of condensate formation and is instead linked to promoting multimerization of the AAD. Two, we identify a novel sight of AAD phosphorylation, on T1098, and show that is required for ATR activation. Three, we identify additional, candidate phosphorylation sites, some of which fit the consensus for casein kinase 2, and we show that casein kinase 2 activity is required for the AAD to perform its function. These studies show that multi-site phosphorylation of the AAD is an important component of the mechanism by which TOPBP1 activates ATR.

40 **Key words**

41 TOPBP1, ATR, AAD, CHK1, multi-site phosphorylation, casein kinase 2

42 **1. Introduction**

43 Ataxia telangiectasia and Rad3-related (ATR) kinase is a vital component of
44 the cellular response to replication stress and DNA damage (Salvidar et al, 2017;
45 Waterman et al, 2020). ATR is also important for the proper timing of cell cycle
46 progression under unperturbed conditions (Saldivar et al, 2018). This large
47 phosphatidylinositol 3-kinase-like kinase (PIKK) is hyper-activated at sites of DNA
48 damage and it goes on to phosphorylate hundreds of substrates to allow cells to
49 survive genotoxic stress. ATR signaling is also a barrier to cancer as it will drive
50 damaged cells into senescence, thereby preventing their continued proliferation
51 (Bartkova et al. 2006; Di Micco et al. 2006). Despite the importance of ATR signaling
52 to human health and disease, it remains unclear how ATR is activated by damaged
53 DNA or stalled replication forks.

54

55 So far, two proteins have been identified that help activate ATR at sites of
56 damage, TOPBP1 and ETAA1 (reviewed in Niedzwiedz, 2016; Salvidar et al, 2017).
57 The work presented here focuses on TOPBP1, which is composed of nine BRCT
58 domains and a discrete and stand-alone ATR activation domain (AAD; Figure 1A). To
59 initiate DNA damage signaling, for example at sites of DNA double-strand breaks
60 (DSBs), ATR is recruited to the DSB via its binding partner ATRIP while TOPBP1 is
61 recruited separately, via an unknown mechanism. At the DSB, TOPBP1 undergoes a
62 conformational change that allows its AAD to contact ATR and ATRIP, in a manner
63 that greatly stimulates ATR kinase activity. Recent work from our group, and others,
64 has revealed that the conformational change is linked to multimerization of TOPBP1

65 at sites of damage (Kim et al, 2020; Thada et al, 2021; Ruis et al, 2021). Notably,
66 while the AAD by itself can activate ATR when present at high concentrations,
67 forced multimerization of the AAD renders it a far more potent activator (Kim et al,
68 2020; Thada et al, 2021). Indeed, forced multimerization of the full-length TOPBP1
69 protein also produces more robust ATR activation (Zhou et al, 2013). These studies
70 make it clear that the way TOPBP1 is regulated is through control of its oligomeric
71 state; TOPBP1 only assumes a multimeric state when it is bound to damaged DNA,
72 and thus ATR is only activated at sites of damage and is not constitutively activated
73 in solution.
74
75 These findings have now focused attention on how TOPBP1 multimers form
76 at sites of damage. Recent work from our group has shed light on this with the
77 derivation of a synthetic form of TOPBP1 that is a stripped-down version lacking all
78 sequences irrelevant to ATR signaling (Ruis et al, 2021). This protein, termed
79 TOPBP1 Jr, contains (1) the first three BRCT domains, which are needed for
80 recruitment to DSBs, (2) the AAD, and (3) the final two BRCT domains, which are
81 required for multimerization (Figure 1A). Other works have shown that sequences
82 within the AAD itself are important for regulation of TOPBP1. For example, it has
83 been shown that serine 1131 in Xenopus TOPBP1 must be phosphorylated by the
84 ataxia telangiectasia mutated (ATM) kinase in order for TOPBP1 to activate ATR
85 (Yoo et al, 2007). Other, more recent work has suggested that phosphorylation of
86 this same serine residue in human TOPBP1 causes the protein to undergo liquid-
87 liquid phase separation to create TOPBP1 condensates at sites of damage (Frattini et

88 al, 2021). These condensates are micron-sized, contain millions of TOPBP1
89 molecules, and are proposed to amplify ATR signaling.
90
91 In this work we use our DSB-mediated ATR activation in *Xenopus* egg extract
92 system (DMAX; Montales et al, 2021; Ruis et al, 2022; Montales et al, 2022) to study
93 how TOPBP1's AAD is regulated. DMAX offers several powerful advantages for
94 mechanistic studies of ATR signaling. For example, ATR signaling is readily assessed
95 by scoring for phosphorylation of the key ATR substrate CHK1. Recruitment to DSBs
96 is also directly assayed in DMAX using DSBs that are immobilized on magnetic beads
97 in a pull-down assay. Structure-function analysis is another key feature of DMAX as
98 target proteins can be removed from *Xenopus* egg extract (XEE) via
99 immunodepletion and mutant forms, rapidly and easily produced by *in vitro*
100 transcription and translation (IVTT), are added back for phenotypic assessment.
101 Using DMAX, we show here that S1131 in the AAD plays an important role in
102 TOPBP1 multimerization independently of condensate formation. We also identify a
103 novel site of phosphorylation within the AAD, T1098, and show that this residue is
104 required for ATR activation. Lastly, we provide evidence that casein kinase 2 is
105 required for ATR activation.
106

107 **2. Material and Methods**

108 *2.1 Materials*

109 *2.1.1 Plasmids*

110 All plasmids used in this study are described below, in table format, and all are

111 *Xenopus* proteins. Specific details about plasmid construction are available upon

112 request.

113

Plasmid	Name	Vector	AA coordinates
5Xmyc-TOPBP1	Cut5	pCS2+MT	1-1513
5Xmyc-TOPBP1 S1131A	pSY29	pCS2+MT	1-1513
5Xmyc-TOPBP1 T1098A	pHS60	pCS2+MT	1-1513
5Xmyc-AAD-BRCT7&8	pHG133	pCS2+MT	971-1513
5Xmyc-TOPBP1 Jr	pKM116	pCS2+MT	1-333 & 992-1513
5Xmyc-AAD	pHG130	pCS2+MT	971-1279
5Xmyc-BRCT7&8	pKM1	pCS2+MT	1235-1470
GST-AAD	pHG117	pGEX-4T3	971-1279
GST-AAD S1131A	pKR10	pGEX-4T3	971-1279
GST-AAD S1131D	pKR11	pGEX-4T3	971-1279
GST-AAD-BRCT7&8	pKR32	pGEX-4T3	971-1513
GST-BRCT7&8	pHG08	pCS2+MT	1197-1513

114

115 *2.1.2 Recombinant proteins*

116 The recombinant proteins used in this study were GST, GST-AAD (wild type,

117 S1131A, S1131D), GST-BRCT7&8, GST-AAD-0BRCT7&8). All proteins were

118 expressed in *E. coli* BL21(DE3) cells, at 37°C for 4 hours, and all proteins were
119 purified from the soluble fraction according to standard procedures (detailed
120 below).
121
122 *2.1.3 Antibodies*
123 We used the following commercially sourced antibodies in this work: Myc
124 (Millipore Sigma #M4439) and GST (Millipore Sigma #05-782). We also used our
125 own antibody against *Xenopus* TOPBP1, HU142, which has been described (Van
126 Hatten et al., 2002).
127
128 *2.2 Methods*
129 *2.2.1 Xenopus egg extracts*
130 The high-speed supernatant (HSS) of XEE was used exclusively in this study. HSS
131 was prepared exactly as described (Smythe and Newport, 1991). For
132 immunodepletion of TOPBP1, the HU142 antibody was used and the procedure was
133 performed exactly as described (Van Hatten et al, 2002). Depleted XEEs were then
134 supplemented with IVTT- produced proteins (2.5 µl IVTT lysate in 20 ul of XEE) as
135 described (Montales et al, 2021).
136
137 *2.2.2 IVTT production of proteins and determination of protein concentrations*
138 IVTT reactions were performed using the SP6 TnT® Quick Coupled
139 Transcription/Translation System (Promega #L2080) according to the
140 manufacturer's instructions.

141

142 *2.2.3 Recombinant Protein Expression and Purification*

143 Plasmids were transformed in BL21 (DE3) Competent *E. Coli* cells and grown in LB
144 media (GST fusion proteins) or LB media with 0.2% glucose (MBP fusion proteins)
145 with ampicillin. At an OD600 of 0.6-0.8, cells were induced with 0.3 mM IPTG for 4
146 hours at 37˚C. Cells were then harvested by centrifugation (4000 rpm for 20 min)
147 and washed with phosphate-buffered saline (PBS). Cells were lysed by sonication in
148 GST column buffer (40% PBS, 60% TEN buffer: 10 mM Tris-Cl, pH 8.0, 1 mM EDTA,
149 pH 8.0, 100 mM NaCl) supplemented with cOmplete protease inhibitor cocktail
150 tablets (Roche #04693159001) and 10 mg lysozyme. Lysates were cleared by
151 centrifugation (15,000 rcf for 20 min) and incubated with glutathione sepharose
152 (BioVision #6566) for 1 hour at 4˚C. Beads were poured over a column and washed
153 with column buffer. GST fusion proteins were eluted with 20 mM glutathione in 75
154 mM HEPES, pH 7.5, 150 mM NaCl, 5 mM DTT, and 0.1% Triton-X. Proteins were
155 dialyzed overnight into PBS.

156

157 *2.2.4 ATR activation (DMAX) assays*

158 For DMAX assays, okadaic acid was first mixed with 20 µl of HSS to a final
159 concentration of 1 µM, as described (Montales et al, 2021). Linear dsDNA derived
160 from EcoRI-digested lambda DNA (Montales et al, 2021) was then added to the
161 mixture and reactions were incubated at room temperature for 30 min. Samples
162 were analyzed via Western blotting using standard conditions. In some cases, when
163 GST-AAD proteins were used, then no DNA was included in the assay. For the

164 experiments shown in Figure 4, the casein kinase 2 inhibitor CX-4945 was used, and
165 it was purchased from Selleckchem.com (catalog # S2248).
166
167 *2.2.5 DSB binding assay.*
168 These were performed exactly as described (Montales et al, 2021). Briefly, a 5 kb
169 PCR fragment was biotinylated via inclusion of a biotin moiety on the forward PCR
170 primer. After PCR and cleanup, the 5 kb PCR fragment was coupled to magnetic
171 streptavidin beads (Dyna- beads M-270 Streptavidin, ThermoFisher) according to
172 the manufacturer's instructions. These "DSB beads", containing 600 fmol of dsDNA
173 per assay, were then incubated in 20 µl of HSS supplemented with 5 µl of an IVTT
174 reaction programmed to produce the protein of interest. After incubation the beads
175 were collected on a magnetic stand and washed three times in PBS + 0.1% TritionX-
176 100. Bound proteins were then eluted with 2X SDS-PAGE sample buffer and
177 examined by Western blotting.
178
179 *2.2.6 Protein binding assays*.
180 For the GST pull-down assays, 5–10 ug of GST fusion proteins were bound to
181 glutathione sepharose beads (BioVision #6566) in Binding Buffer (PBS + 0.1 % NP-
182 40) for one hour at 4◦C and then the beads were washed with Binding Buffer. Next,
183 20 µL of IVTT proteins were diluted into 400 µL of Binding Buffer and then
184 incubated with the washed beads for one hour at 4◦C. The beads were washed four
185 times with 500 µL of Binding Buffer and then eluted with 2X Sample Buffer

186 (Millipore Sigma #S3401-10VL). The input and bound fractions were then analyzed
187 via Western blotting using standard conditions.
188
189 *Mass spectrometry analysis of GST-AAD*
190 GST-AAD was incubated in XEE for 30 minutes at room temperature and purified
191 back out of the extract via glutathione-sepharose affinity chromatography. The
192 sample was run on SDS-PAGE and a Coomassie-stained band was excised from the
193 gel. Proteins in coomassie-stained gel slices were reduced, alkylated and digested by
194 trypsin as previously described (Kaiser and Wohlschlegel, 2005). After digestion,
195 peptides were extracted from the gel slices using 100 µl of 60% acetonitrile/0.1%
196 TFA, dried in a SpeedVac vacuum concentrator, desalted using C18 tips, and
197 reconstituted in 10 µl of 5% formic acid for LC-MS/MS analysis.
198 Desalted peptide mixtures were loaded onto a 25 cm long, 75 µm inner diameter
199 fused-silica capillary, packed in-house with bulk 1.9 µM ReproSil-Pur beads with
200 120 Å pores as described previously (Jami-Alahmadi et al, 2021). Peptides were
201 analyzed using a 140 min water-acetonitrile gradient delivered by a Dionex Ultimate
202 3000 UHPLC (Thermo Fisher Scientific) operated initially at 400 nL/min flow rate
203 with 1% buffer B (acetonitrile solution with 3% DMSO and 0.1% formic acid) and
204 99% buffer A (water solution with 3% DMSO and 0.1% formic acid). Buffer B was
205 increased to 6% over 5 min at which time the flow rate was reduced to 200 nl/min.
206 A linear gradient from 6-28% B was applied to the column over the course of 123
207 min. The linear gradient of buffer B was then further increased to 28-35% for 8 min
208 followed by a rapid ramp-up to 85% for column washing. Eluted peptides were

209 ionized via a Nimbus electrospray ionization source (Phoenix S&T) by application of
210 a distal voltage of 2.2 kV.
211
212 All mass spectrometry data were collected using data dependent acquisition on
213 Orbitrap Fusion Lumos Tribrid mass spectrometer (Thermo Fisher Scientific) with
214 an MS1 resolution of 120,000 followed by sequential MS2 scans at a resolution of
215 15,000. The Integrated Proteomics pipeline 2 was utilized to generate peptide and
216 protein identifications. MS2 spectra were searched using the ProLuCID algorithm
217 against the Xenopus reference proteome (xenbase.org) followed by filtering by
218 DTASelect using a decoy database estimated false discovery rate of < 1% (Xu et al,
219 2015; Cociorva et al, 2007).

220 **3. Results and Discussion**

221 *3.1 Serine 1131 promotes TOPBP1's ability to activate ATR in a manner independent of*
222 *condensate formation.*

223 Previous work from the Dunphy group had identified S1131 in TOPBP1's
224 AAD as an ATM phospho-acceptor site that is required for ATR activation in XEE
225 under some conditions (Yoo et al, 2007). S1131 is required for ATR activation by
226 small homopolymeric oligonucleotides like A_{70}-T_{70} (AT70), and by sperm chromatin
227 digested with EcoRI to produce DSBs. Interestingly, S1131 is dispensable for ATR
228 activation by stalled replication forks. We thus initiated our studies by checking the
229 requirement for S1131 in our DMAX system. To do so, we performed
230 immunodepletion, where either non-specific or anti-TOPBP1 antibodies are coupled
231 to Protein A beads and then incubated with XEE. After incubation, the XEE is
232 recovered away from the antibody beads containing the captured TOPBP1 and used
233 for ATR activation assays. EcoRI-digested λ DNA was used as a source of DSBs. We
234 also prepared recombinant forms of TOPBP1, using IVTT in rabbit reticulocyte
235 lysates, so that they could be added back to the depleted extracts. As shown in
236 Figure 1B, a mock-depleted extract (treated with non-specific antibody beads, lane
237 1, labeled "TOPBP1$^+$ XEE") contained TOPBP1 and was able to activate ATR. By
238 contrast, for the TOPBP1-depleted extract, TOPBP1 levels were substantially
239 reduced, and this extract was deficient for ATR activation (Figure 1B, lane 2). When
240 wild type TOPBP1 was added back to the TOPBP1-depleted extract, then ATR
241 activation was restored (lane 3), and this did not occur when an S1131A mutant
242 form of TOPBP1 was added back (lane 4). This experiment shows that S1131 is

243 required for ATR activation by TOPBP1 in our DMAX system. Previous work had not
244 addressed if S1131 is important for TOPBP1 recruitment to DSBs, and thus we
245 employed our DSB binding assay to examine this important issue. DSB beads were
246 prepared as previously described (Montales et al, 2021), where linear, 5kb dsDNAs
247 with biotin moieties attached to end are immobilized on magnetic streptavidin
248 beads. The beads are then incubated in XEE containing myc-tagged forms of either
249 wild type or S1131A TOPBP1. Since our previous work has repeatedly shown that
250 TOPBP1 does not bind to streptavidin beads lacking DNA under these assay
251 conditions (Montales et al, 2021; Ruis et al, 2022; Montales et al, 2022), we did not
252 include empty beads in this experiment. After incubation, the beads were isolated,
253 washed, and probed for TOPBP1 occupancy by Western blotting. As shown in Figure
254 1C, both wild type and S1131A TOPBP1 could bind to DSBs. We conclude S1131 is
255 dispensable for recruitment of TOPBP1 to DSBs, and likely functions after
256 recruitment to stimulate DNA-bound ATR kinase.
257
258 What is the role of S1131 in ATR activation? Previous work has shown that
259 phosphorylation of S1131 (to produce P-S1131) makes binding of TOPBP1 to ATR-
260 ATRIP more efficient (Yoo et al, 2007). More recently, it has been shown for human
261 TOPBP1 that P-S1138, the analogous residue, is required for TOPBP1's ability to
262 phase separate (Frattini et al, 2021). This, in turn, promotes robust ATR signaling.
263 Importantly, although the human AAD contains S1138, the AAD by itself cannot
264 undergo phase transition as additional sequences are required (Frattini et al, 2021).
265 The AAD by itself can, however, activate ATR when added as a GST fusion protein to

266 XEE (Kumagai et al, 2006). Given these circumstances, we reasoned that if S1131
267 functions exclusively in the context of condensate formation then it should be
268 irrelevant to the ability of the isolated AAD, which cannot form a condensate, to
269 activate ATR. To put this notion to the test, we prepared GST-AAD fusion proteins of
270 three types: wild type, S1131A, and S1131D. Previous work has shown that the
271 S1131D substitution, which mimics P-S1131, produces a dominant, gain-of-function
272 TOPBP1 that binds ATR-ATRIP more efficiently and activates ATR more readily (Yoo
273 et al, 2007). This previous work did not, however, test the S1131D mutation in the
274 context of the isolated AAD. The three different GST-AAD proteins were added to
275 XEE at the indicated concentrations and ATR signaling was assessed by anti P-CHK1
276 Western blotting (Figure 1D). The S1131A mutant produced less P-CHK1 than did
277 the wild type version when both were present at 4 uM (compare lanes 2 and 4 in
278 Figure 1D). This shows that S1131 is important for the ability of the isolated AAD to
279 activate ATR, and thus that S1131 can function independently of condensate
280 formation to promote ATR signaling. Interestingly, we observed the opposite effect
281 for the S1131D mutation which hyper-activated ATR (compare lanes 2 and 5 in
282 Figure 1D). This is consistent with previous data showing that S1131D in the
283 context of full-length TOPBP1 promotes ectopic activation of ATR (Yoo et al, 2007),
284 and our data extend these previous data by showing that S1131D can exert this
285 effect in the context of the AAD alone. Based on the data in Figure 1, we conclude
286 that the ability of S1131 to promote ATR activation is an intrinsic property of the
287 AAD, and thus can be disconnected from condensate formation. This is not to say

288 that it is not involved in condensate formation, but it is clearly doing something
289 separate from phase transition.
290
291 *3.2 S1131 promotes TOPBP1 multimerization.*
292 In recent work we used a synthetic form of TOPBP1, TOPBP1 Jr, to show that
293 just three functional domains are needed for regulated activation of ATR by TOPBP1
294 (Ruis et al, 2021). The BRCT0-2 domains mediate recruitment and are dispensable
295 thereafter while the AAD interfaces with ATR-ATRIP and the BRCT7&8 domains
296 promote multimerization in an unknown manner. To determine if S1131 is possibly
297 connected to TOPBP1 multimerization we first asked if the BRCT7&8 domains of
298 TOPBP1 could interact with the AAD. For this, a standard GST pull-down assay and
299 the GST fusion proteins we used are shown in Figure 2A. These proteins were used
300 in binding assays with myc-tagged BRCT7&8, produced by IVTT. As shown in Figure
301 2B, myc-BRCT7&8 did not bind to GST alone, but did bind to GST-AAD, GST-
302 BRCT7&8, and a fragment containing both the AAD and BRCT7&8. We next
303 examined how the same set of GST proteins would bind to myc-tagged AAD alone,
304 and again detectable binding was observed for all of the GST fusions but not GST
305 alone (Figure 2C). In this experiment, however, the binding efficiencies differed,
306 with the more efficient binding observed for GST-BRCT7&8, less efficient binding to
307 GST-AAD-BRCT7&8, and relatively weak binding to GST-AAD. These data show that
308 the AAD domain interacts with itself weakly, and that it binds BRCT7&8 more
309 robustly (Figure 2D). In addition, the data show that BRCT7&8 can self-associate.

310 We note that others have previously shown that the AAD can interact with itself
311 (Thada et al, 2019).
312
313 To pursue these observations, we next asked how S1131 would impact
314 interaction of the ADD with the TOPBP1 Jr. We chose TOPBP1 Jr for this analysis
315 because, unlike the other constructs, TOPBP1 Jr has been shown to activate ATR in
316 the context of DSBs (Ruis et al, 2021). We used the same GST proteins for this
317 experiment as were used in Figure 1D. As shown in Figure 2E, myc-tagged TOPBP1
318 Jr could bind to the wild type AAD, and binding was somewhat reduced with the
319 S1131A mutant. Interestingly, binding was increased, relative to wild type, with the
320 S1131D mutant. Thus the same phospho-mimic mutation that increases ATR
321 activation by the AAD also increases multimerization. We conclude that promoting
322 multimerization is a previously undisclosed function of S1131.
323
324 *3.3 T1098 within the AAD is phosphorylated in XEE and required for ATR activation.*
325 During the course of our studies of TOPBP1's AAD, we noticed that, after
326 incubation in XEE, that GST-AAD protein migrated with reduced mobility on SDS-
327 PAGE. This can be seen in Figure 3A, where GST-AAD that had been incubated in
328 XEE and then recovered back out of the extract using glutathione sepharose beads
329 was run side-by-side with the input material. This reduced mobility suggests that
330 post-translational modifications (PTMs) had been placed on GST-AAD during
331 incubation in XEE, and thus to gain a sense of what these PTMs are we excised the
332 band in Figure 3A, lane 3, and submitted it to analysis by mass spectrometry. This

333 analysis revealed several peptides containing phosphorylated serine or threonine
334 residues (Figure 3B). Figure 3C shows the sequence of the AAD from *Xenopus*
335 TOPBP1 and these candidate phospho-acceptor sites are highlighted in red. The
336 underlined portion shows the region in the frog protein that corresponds to the
337 minimally defined AAD from human TOPBP1 (Thada et al, 2019), and thus two of
338 the candidate phospho-acceptor sites (S1095 and T1098) fall within this region. We
339 note that S1131 is only phosphorylated during a DNA damage response (Yoo et al,
340 2007), and thus we did not expect to recover P-S1131 signals in this experiment.
341
342 To pursue these observations, we next asked two questions – are the
343 candidate phospho-acceptor sites identified by the mass spectrometry analysis
344 conserved in human TOPBP1 and, if so, have any of those sites been curated on the
345 website PhosphoSitePlus® (www.phosphosite.org), which catalogs phospho-sites
346 for all human proteins? The answers are displayed in Figure 3D, where seven of the
347 nine sites identified by mass spectrometry are conserved in human TOPBP1 and
348 two of these, S1008 and T1098, are listed on PhosphoSitePlus®. Because T1098 is
349 conserved in humans, listed on PhosphoSitePlus®, and falls within the minimally
350 defined AAD, we focused on it first. The MS/MS spectrum for the peptide harboring
351 pT1098 is displayed in Figure 4A. To determine if this residue is important for ATR
352 activation, we produced a T1098A point mutant in full-length TOPBP1 and we
353 tested this mutant for ATR activation, exactly as we did for S1131 in Figure 1B. As
354 shown in Figure 4B, the T1098A mutant fails to activate ATR. This result shows that

355 S1131 is not the only critical phospho-acceptor site within the AAD, as T1098 is also
356 important.
357
358 *3.4 A casein kinase 2 inhibitor blocks both DSB- and ADD-mediated ATR activation.*
359 One feature of the AAD region of TOPBP1 is that it contains an unusually high
360 number of consensus sequences for phosphorylation by casein kinase 2. The
361 consensus motif for casein kinase 2 is S/T-X-X-D/E (St-Denis et al, 2015), and this
362 motif is found nine times in the AAD region (Figure 5A), and one of these (S1266)
363 was identified in our mass spectrometry analysis and is conserved in human
364 TOPBP1. This prompted us to ask if casein kinase 2 activity is required for the AAD
365 to function. For this, we asked if DSBs could still activate ATR in XEEs treated with
366 the casein kinase 2 inhibitor (CK2i) CX-4945. We found that CX-4945 could block
367 ATR activation (Figure 5B). We have previously shown that CX-4945 does not
368 impair the recruitment of TOPBP1 to DSBs (Montales et al, 2022) and thus we
369 considered the possibility that the AAD requires casein kinase 2 activity in order to
370 function. To test this idea we added GST-AAD to XEE and observed that CX-4945
371 could still inhibit ATR activation. Based on this experiment, we conclude that the
372 AAD requires, either directly or indirectly, casein kinase 2 activity in order to
373 activate ATR.
374
375 In this paper we present data showing that phosphorylation of TOPBP1's
376 AAD is crucial for its ability to activate ATR. Previous work had identified S1131 as a
377 regulated phospho-acceptor site necessary for ATR activation by DSBs, but not

378 stalled replication forks. This previous work showed that S1131 is phosphorylated
379 by ATM, and that the manifestation of this phosphorylation was increased affinity
380 for ATR-ATRIP (Yoo et al, 2007). Here, we extend these observations by showing
381 that S1131 is important for multimerization of the AAD (Figure 3E). We also report
382 that an additional residue within the AAD, T1098, is also phosphorylated, but this is
383 constitutive phosphorylation as it occurs in the absence of a DDR response. Like
384 S1131, phosphorylation of T1098 is required for ATR activation. Summarizing these
385 findings, we see that under resting conditions, TOPBP1 is primed for action via
386 constitutive phosphorylation on T1098; however in its monomeric form, it is unable
387 to activate ATR (Figure 7). ATM-directed phosphorylation of S1131 occurs in
388 response to DSBs, and now TOPBP1 can assume the multimeric form that is
389 required for ATR activation (Figure 7). It is likely that additional sites within the
390 AAD are also phosphorylated, as this region contains multiple casein kinase 2
391 consensus motifs and we have shown here that casein kinase 2 activity is required
392 for AAD function (Figure 6). In conclusion, our data show that the AAD undergoes
393 multi-site phosphorylation, under both constitutive and regulated conditions, and
394 that at least some of these phosphorylations convert TOPBP1 from an inactive to an
395 active form via multimerization.

396 **Author contribution**

397 W.M.M. conceptualized the project, acquired the funding, and wrote the manuscript.

398 H.S., K.R., and K.M. performed the experiments. J.A.W. and Y.J. performed the mass

399 spectrometry experiments.

400

401 **Conflict of interest statement**

402 The authors declare no conflict of interest.

403

404 **Acknowledgments**

405 This work was supported by NIH grant R01GM12287 (W.M.M.) and R01GM089778

406 (J.A.W.). We thank Shan Yan and Hovik Gasparyan for the production of plasmid

407 constructs used in this study.

408 **References**
409
410 Bartkova J, Rezaei N, Liontos M, Karakaidos P, Kletsas D, Issaeva N, Vassiliou LV,
411 Kolettas E, Niforou K, Zoumpourlis VC, Takaoka M, Nakagawa H, Tort F, Fugger K,
412 Johansson F, Sehested M, Andersen CL, Dyrskjot L, Ørntoft T, Lukas J, Kittas C,
413 Helleday T, Halazonetis TD, Bartek J, Gorgoulis VG. Oncogene-induced senescence is
414 part of the tumorigenesis barrier imposed by DNA damage checkpoints. Nature.
415 2006 Nov 30;444(7119):633-7. doi: 10.1038/nature05268. PMID: 17136093.
416
417 Cociorva D, L Tabb D, Yates JR. Validation of tandem mass spectrometry database
418 search results using DTASelect. Curr Protoc Bioinformatics. 2007 Jan;Chapter
419 13:Unit 13.4. doi: 10.1002/0471250953.bi1304s16. PMID: 18428785.
420
421 Di Micco R, Fumagalli M, Cicalese A, Piccinin S, Gasparini P, Luise C, Schurra C, Garre'
422 M, Nuciforo PG, Bensimon A, Maestro R, Pelicci PG, d'Adda di Fagagna F. Oncogene-
423 induced senescence is a DNA damage response triggered by DNA hyper-replication.
424 Nature. 2006 Nov 30;444(7119):638-42. doi: 10.1038/nature05327. PMID:
425 17136094.
426
427 Frattini C, Promonet A, Alghoul E, Vidal-Eychenie S, Lamarque M, Blanchard MP,
428 Urbach S, Basbous J, Constantinou A. TopBP1 assembles nuclear condensates to
429 switch on ATR signaling. Mol Cell. 2021 Mar 18;81(6):1231-1245.e8. doi:
430 10.1016/j.molcel.2020.12.049. Epub 2021 Jan 26. PMID: 33503405.
431
432 Jami-Alahmadi Y, Pandey V, Mayank AK, Wohlschlegel JA. A Robust Method for
433 Packing High Resolution C18 RP-nano-HPLC Columns. J Vis Exp. 2021 May 14;(171).
434 doi: 10.3791/62380. PMID: 34057454.
435
436 Kaiser P, Wohlschlegel J. Identification of ubiquitination sites and determination of
437 ubiquitin-chain architectures by mass spectrometry. Methods Enzymol.
438 2005;399:266-77. doi: 10.1016/S0076-6879(05)99018-6. PMID: 16338362.
439
440 Kim A, Montales K, Ruis K, Senebandith H, Gasparyan H, Cowan Q, Michael WM.
441 Biochemical analysis of TOPBP1 oligomerization. DNA Repair (Amst). 2020
442 Dec;96:102973. doi: 10.1016/j.dnarep.2020.102973. Epub 2020 Sep 21. PMID:
443 32987353; PMCID: PMC7670859.
444
445 Kumagai A, Lee J, Yoo HY, Dunphy WG. TopBP1 activates the ATR-ATRIP complex.
446 Cell. 2006 Mar 10;124(5):943-55. doi: 10.1016/j.cell.2005.12.041. PMID: 16530042.
447
448 Montales K, Kim A, Ruis K, Michael WM. Structure-function analysis of TOPBP1's
449 role in ATR signaling using the DSB-mediated ATR activation in Xenopus egg
450 extracts (DMAX) system. Sci Rep. 2021 Jan 11;11(1):467. doi: 10.1038/s41598-020-
451 80626-1. PMID: 33432091; PMCID: PMC7801695.
452

453 Montales K, Ruis K, Lindsay H, Michael WM. MRN-dependent and independent
454 pathways for recruitment of TOPBP1 to DNA double-strand breaks. PLoS One. 2022
455 Aug 2;17(8):e0271905. doi: 10.1371/journal.pone.0271905. PMID: 35917319;
456 PMCID: PMC9345342.
457
458 Niedzwiedz W. Activating ATR, the devil's in the dETAA1l. Nat Cell Biol. 2016 Oct
459 27;18(11):1120-1122. doi: 10.1038/ncb3431. Erratum in: Nat Cell Biol. 2016 Nov
460 29;18(12):1367. PMID: 27784903.
461
462 Ruis K, Huynh O, Montales K, Barr NA, Michael WM. Delineation of a minimal
463 topoisomerase II binding protein 1 for regulated activation of ATR at DNA double-
464 strand breaks. J Biol Chem. 2022 Jul;298(7):101992. doi:
465 10.1016/j.jbc.2022.101992. Epub 2022 Apr 28. PMID: 35490781; PMCID:
466 PMC9257406.
467
468 Saldivar JC, Cortez D, Cimprich KA. The essential kinase ATR: ensuring faithful
469 duplication of a challenging genome. Nat Rev Mol Cell Biol. 2017 Oct;18(10):622-
470 636. doi: 10.1038/nrm.2017.67. Epub 2017 Aug 16. Erratum in: Nat Rev Mol Cell
471 Biol. 2017 Dec;18(12):783. PMID: 28811666; PMCID: PMC5796526.
472
473 Saldivar JC, Hamperl S, Bocek MJ, Chung M, Bass TE, Cisneros-Soberanis F, Samejima
474 K, Xie L, Paulson JR, Earnshaw WC, Cortez D, Meyer T, Cimprich KA. An intrinsic
475 S/G2 checkpoint enforced by ATR. Science. 2018 Aug 24;361(6404):806-810. doi:
476 10.1126/science.aap9346. PMID: 30139873; PMCID: PMC6365305.
477
478 Smythe C, Newport JW. Systems for the study of nuclear assembly, DNA replication,
479 and nuclear breakdown in Xenopus laevis egg extracts. Methods Cell Biol.
480 1991;35:449-68. doi: 10.1016/s0091-679x(08)60583-x. PMID: 1664032.
481
482 St-Denis N, Gabriel M, Turowec JP, Gloor GB, Li SS, Gingras AC, Litchfield DW.
483 Systematic investigation of hierarchical phosphorylation by protein kinase CK2. J
484 Proteomics. 2015 Apr 6;118:49-62. doi: 10.1016/j.jprot.2014.10.020. Epub 2014
485 Nov 5. PMID: 25449829.
486
487 Thada V, Cortez D. Common motifs in ETAA1 and TOPBP1 required for ATR kinase
488 activation. J Biol Chem. 2019 May 24;294(21):8395-8402. doi:
489 10.1074/jbc.RA119.008154. Epub 2019 Apr 2. PMID: 30940728; PMCID:
490 PMC6544864.
491
492 Thada V, Cortez D. ATR activation is regulated by dimerization of ATR activating
493 proteins. J Biol Chem. 2021 Jan-Jun;296:100455. doi: 10.1016/j.jbc.2021.100455.
494 Epub 2021 Feb 24. PMID: 33636182; PMCID: PMC7994790.
495
496 Van Hatten RA, Tutter AV, Holway AH, Khederian AM, Walter JC, Michael WM. The
497 Xenopus Xmus101 protein is required for the recruitment of Cdc45 to origins of
498 DNA replication. J Cell Biol. 2002 Nov 25;159(4):541-7. doi:

10.1083/jcb.200207090. Epub 2002 Nov 18. PMID: 12438414; PMCID: PMC2173091.

Waterman DP, Haber JE, Smolka MB. Checkpoint Responses to DNA Double-Strand Breaks. Annu Rev Biochem. 2020 Jun 20;89:103-133. doi: 10.1146/annurev-biochem-011520-104722. Epub 2020 Mar 16. PMID: 32176524; PMCID: PMC7311309.

Xu T, Park SK, Venable JD, Wohlschlegel JA, Diedrich JK, Cociorva D, Lu B, Liao L, Hewel J, Han X, Wong CCL, Fonslow B, Delahunty C, Gao Y, Shah H, Yates JR 3rd. ProLuCID: An improved SEQUEST-like algorithm with enhanced sensitivity and specificity. J Proteomics. 2015 Nov 3;129:16-24. doi: 10.1016/j.jprot.2015.07.001. Epub 2015 Jul 11. PMID: 26171723; PMCID: PMC4630125.

Yoo HY, Kumagai A, Shevchenko A, Shevchenko A, Dunphy WG. Ataxia-telangiectasia mutated (ATM)-dependent activation of ATR occurs through phosphorylation of TopBP1 by ATM. J Biol Chem. 2007 Jun 15;282(24):17501-6. doi: 10.1074/jbc.M701770200. Epub 2007 Apr 19. PMID: 17446169.

Zhou ZW, Liu C, Li TL, Bruhn C, Krueger A, Min W, Wang ZQ, Carr AM. An essential function for the ATR-activation-domain (AAD) of TopBP1 in mouse development and cellular senescence. PLoS Genet. 2013;9(8):e1003702. doi: 10.1371/journal.pgen.1003702. Epub 2013 Aug 8. PMID: 23950734; PMCID: PMC3738440.

523 **Figures and Legends**

524

525 **Figure 1. S1131 in TOPBP1's AAD is dispensable for recruitment of TOPBP1 to**

526 **DSBs but is required for ATR activation in the DMAX system.**

527 **A.** Schematic representation of full length TOPBP1 and TOPBP1 Junior. **B.** A DMAX

528 assay where XEE was immunodepleted of endogenous TOPBP1 and then

529 supplemented with the indicated IVTT-produced TOPBP1 proteins prior to the

530 addition of DSBs. TOPBP1^{+} XEE (lane 1) refers to extract that was mock-depleted

531 using non-specific IgG. Blank (lane 2) refers to a TOPBP1-depleted extract that

532 received an unprogrammed IVTT reaction. After incubation, the samples were

533 probed by Western blotting for P-CHK1, CHK1, and TOPBP1 (using anti-TOPBP1

534 antibody HU142). The experiment shown is representative of two independently

535 performed biological replicates. **C.** HSS was combined with IVTT-produced and myc-

536 tagged TOPBP1 proteins. These proteins were the wild type form ("WT") and the

537 S1131A mutant. DSB beads were then added and the samples were incubated for 30

538 min. After incubation, the beads were washed and eluted and the samples were

539 probed by Western blot for the indicated protein. The myc antibody was used to

540 probe for TOPBP1. The bound samples were also stained by silver and a 12.5 kDa

541 low molecular weight (l.m.w) protein is shown, to demonstrate equal isolation of the

542 beads. The experiment shown is representative of two independently performed

543 biological replicates. **D.** The indicated GST proteins were added to XEE at the

544 indicated concentrations and incubation was carried out for 30 minutes at room

545 temperature. The samples were then probed for P-CHK1, CHK1, and GST. The

546 experiment shown is representative of two independently performed biological
547 replicates.
548
549 **Figure 2. S1131 is important for multimerization of the AAD.**
550 **A.** Schematic representation of the proteins used for protein binding assays. **B.** The
551 indicated GST proteins, expressed and purified from *E. coli*, were incubated in IVTT
552 reactions expressing myc-tagged BRCT7&8. After incubation the samples were
553 diluted in Binding Buffer and incubated with glutathione-sepharose beads. The
554 beads were then washed, and the samples were eluted and probed by Western
555 blotting for the indicated proteins. A sample of the total binding reaction, taken
556 prior to dilution, was also probed for myc (lane "input"). The experiment shown is
557 representative of two independently performed biological replicates. **C.** Same as
558 (B) except myc-AAD was used. The experiment shown is representative of two
559 independently performed biological replicates. **D.** Schematic showing how the AAD-
560 BRCT7&8 region interacts with itself. **E.** Same as (B) except myc-TOPBP1 Jr was
561 used with the indicated GST fusion proteins. The experiment shown is
562 representative of two independently performed biological replicates.
563
564 **Figure 3. Mass spectrometry reveals multiple phospho-acceptor sies within**
565 **the AAD region.**
566 **A.** A Coomassie blue stained SDS-PAGE gel showing altered mobility of GST-AAD
567 after incubation in XEE. **B.** The amino acid sequence of the AAD region used for
568 mass spectrometry analysis. See main text for details. **C.** Summary of conservation

569 and PhosphoSitePlus® hits for the phospho-acceptor sites identified by mass
570 spectrometry.
571
572 **Figure 4. T1098 is required for ATR activation by TOPBP1.**
573 **A.** MS/MS spectra for the peptide harboring T1098. **B.** Same as Figure 1B except the
574 T1098A mutant was used. The experiment shown is representative of two
575 independently performed biological replicates.
576
577 **Figure 5. Delineation of the NBS1 binding region within TOPBP1's BRCT1**
578 **domain.**
579 **A.** Same as Figure 3C except the position of consensus casein kinase 2
580 phosphorylation sites is highlighted with grey shading. **B-C.** XEEs were treated as
581 indicated with either DMSO or CK2i and either DSBs (B.) or the indicated GST
582 proteins (C.) were added. After incubation the samples were probed by Western
583 blotting for P-CHK1 and CHK1. The experiments shown are representative of two
584 independently performed biological replicates.
585
586 **Figure 6. Multi-site phosphorylation of the TOPBP1 AAD drives ATR activation**
587 **through a multimerization mechanism.**
588 Please see text for details.

589 **Figure 1**

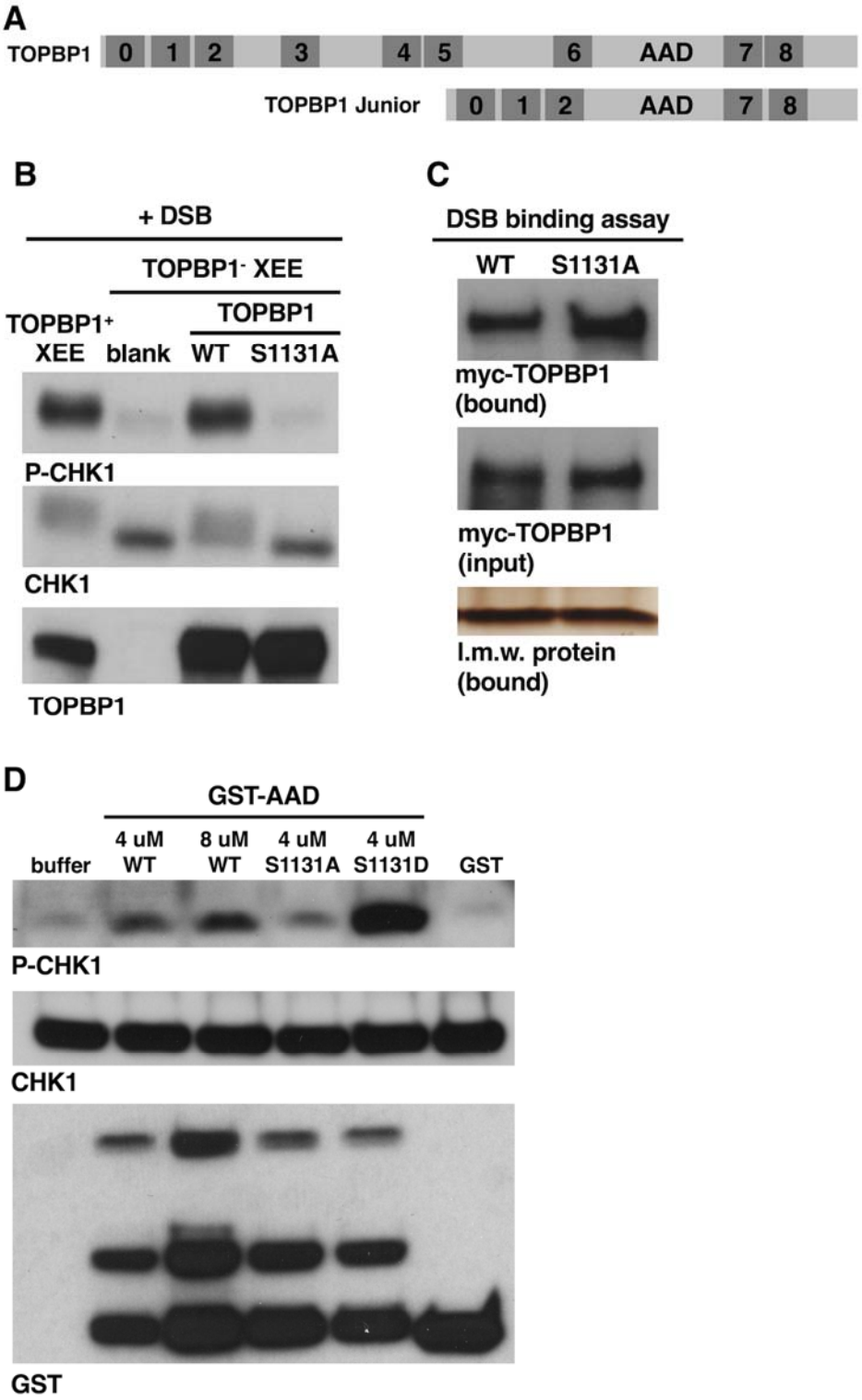

590

591

592 **Figure 2**

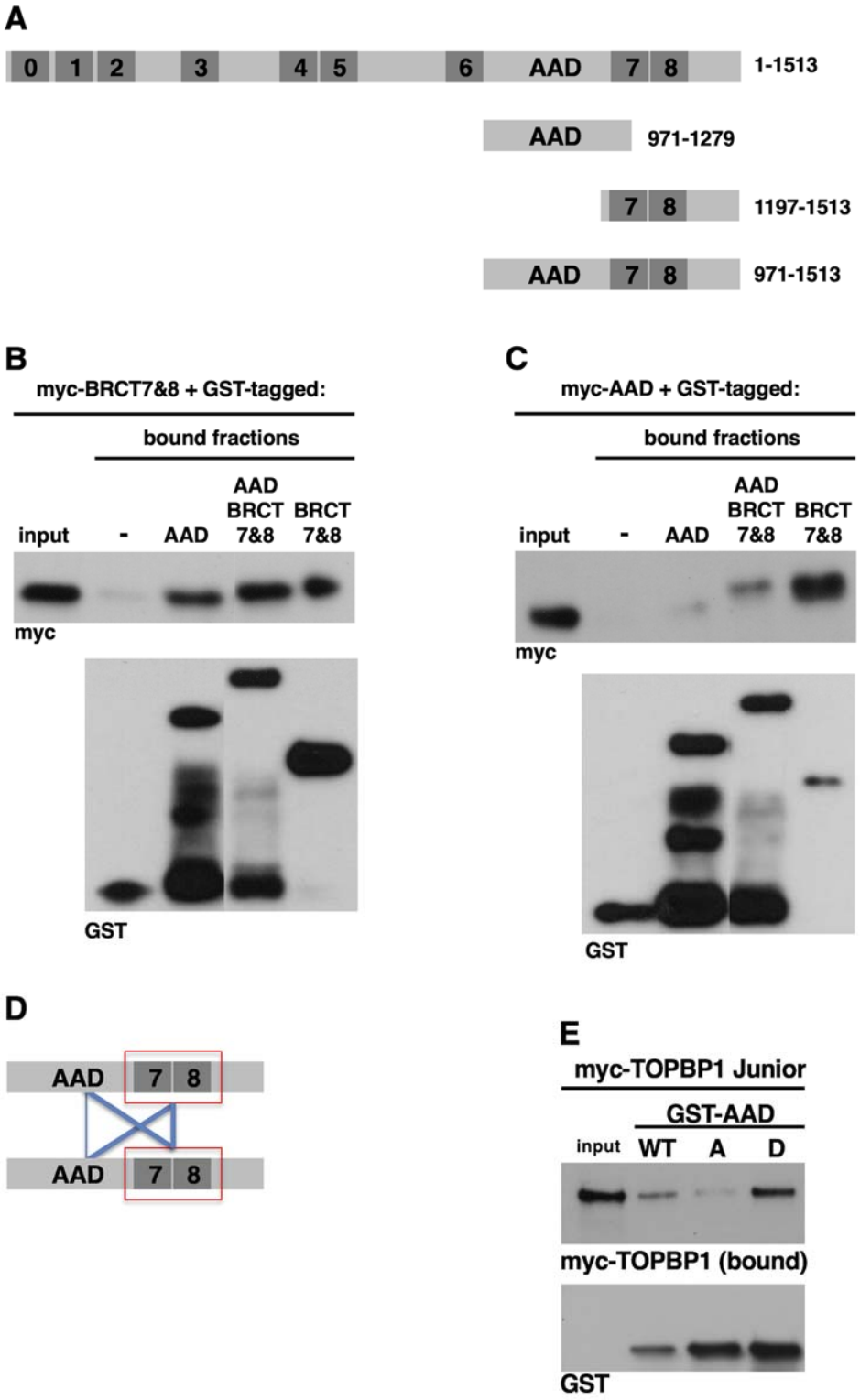

593

594

595 **Figure 3**

A

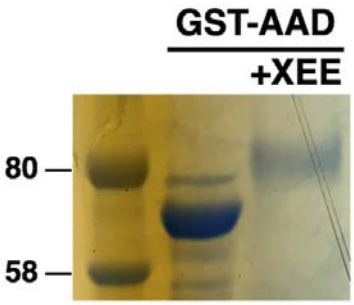

B

^{972}EQQKRVPEALYPHTYNPKMSLDISAVQDGSYTASKFSADTSLQQDENSELQLQQ
NNKFGETSDDQVKKAAGDGNPQNPSKDVKGALTQTLEMRENFQRQLQEFMSATS
VVKPRGSVGRAGFDNSPCTPEGARSTRNGRSRVLEALRQSRQAMTDLNTEPSQNE
QIIWDDPTAREERAKLVSNLQWPDSPSQYSEQLQHNMNDAGGNYTPAKESLTDSEI
AELEACEFEPKSAMRTPVIENNLQSPTKPDHLTPTPQAPSIAFPLANPPVAPQPREK
PVQPFSKEETLKERRFQLSSLDPQERIDYSQL^{1167}

C

frog site	human equivalent	PhosphoSitePlus® hits
S1008	S1016	2
T1011	S1019	0
T1031	not conserved	na
S1095	not conserved	na
T1098	T1105	1
S1266	S1273	0
S1267	S1274	0

596

597

598 **Figure 4**

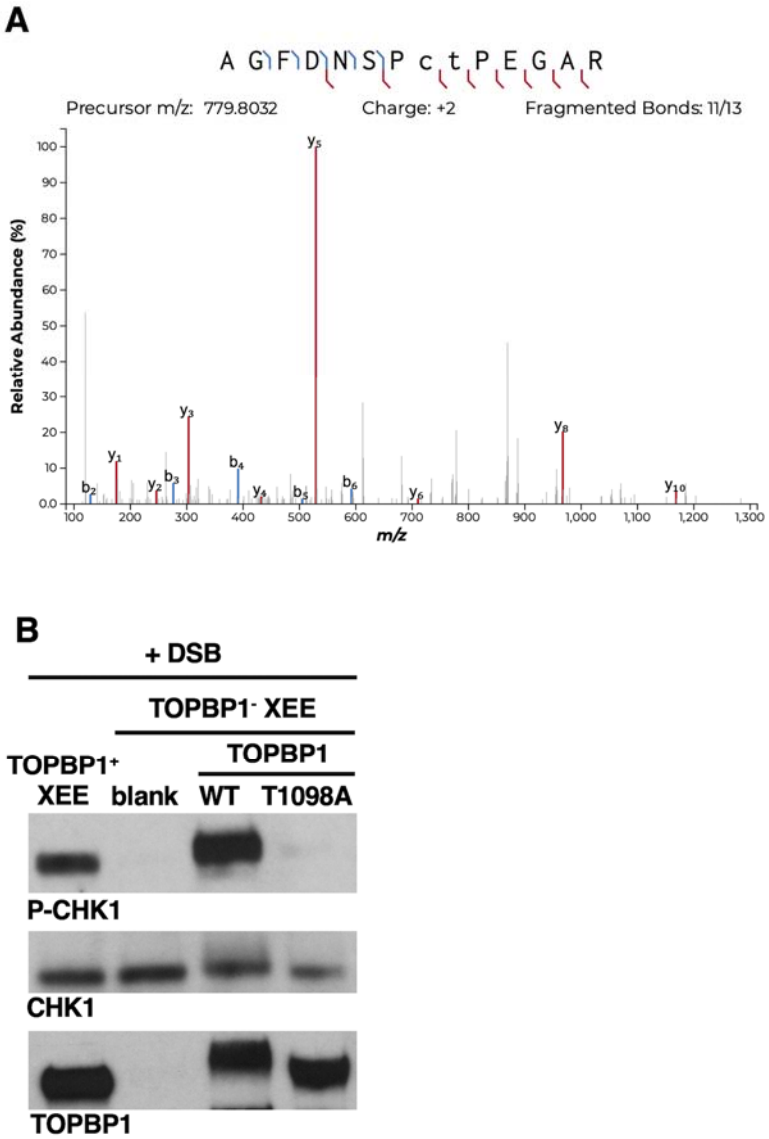

599

600

601 **Figure 5**

602

603

604 **Figure 6**

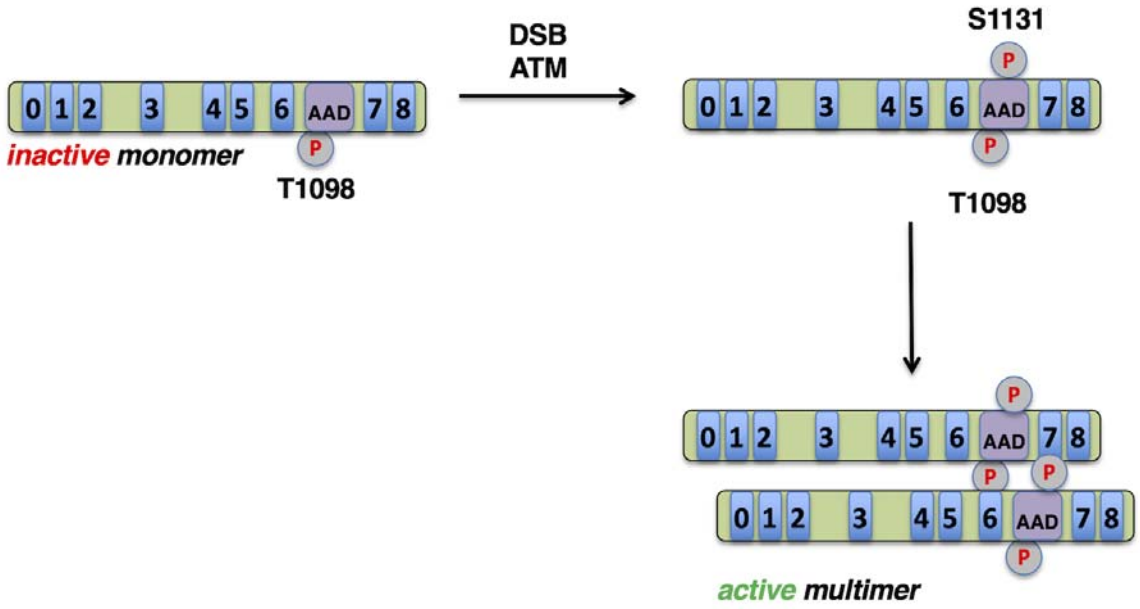

605

606